

Delineation of post-phloem assimilate transport pathway into developing caryopsis
of *Brachypodium distachyon*

Charles Ugochukwu Solomon^{1,2}

Sinead Drea¹

¹Department of Genetics and Genome Biology, University of Leicester, University Road, Leicester
LE1 7RH, UK

²Abia State University, Uturu, PMB 2000 Uturu, Nigeria

Email: cus2@le.ac.uk; sd201@le.ac.uk

Phone: +447835298029

Date of submission:

Number of tables: 0

Number of figures: 4

Word count: 4668

1
2 **Delineation of post-phloem assimilate transport pathway into developing caryopsis**
3 **of *Brachypodium distachyon***

4
5 **Highlights**

- 6
7 • Based on existing work, we propose Caryopsis Endosperm Assimilate Acquisition Route
8 (CEAAR) models, that describes the exact path of assimilate import into caryopsis
9 endosperms.
10
11 • The structure of the post-phloem transfer cells of *Brachypodium distachyon* mirrors
12 temperate and tropical cereals.
13
14
15 • Assimilate delivery into *Brachypodium distachyon* endosperm is identical to assimilate
16 import into rice endosperm.
17

18 **Abstract**

19 Assimilates stored in mature cereal grains are mobilized from source tissues and transported
20 towards developing grains through the vascular bundle. Due to the lack of direct vascular
21 connection between maternal grain vascular bundle and filial tissues, post-phloem transportation of
22 assimilates into grain endosperm relies on transfer cells that lie between the grain vascular bundle
23 and the endosperm. Here, we propose Caryopsis Endosperm Assimilate Acquisition
24 Route (CEAAR) models that describes the exact path of assimilate import into caryopsis
25 endosperms. Using fluorescent tracer dyes we also delineated the route of assimilate delivery into
26 *Brachypodium distachyon* endosperm and classified it as ventral circuitous (vc-CEAAR), an
27 assimilate import model also found in rice. Furthermore, we report a detailed anatomical study of
28 post-phloem assimilate transport pathway in developing grains of *Brachypodium distachyon*. Our
29 results highlight major anatomical similarities and differences between the grain post-phloem
30 transfer cells of *Brachypodium* and those of crop species such as rice, wheat, and barley relevant to
31 post-phloem assimilate transport.
32

33 **Key words;** Assimilate, *Brachypodium*, Cereals, Endosperm, Transfer cells, Transport

34
35 **Abbreviations**

36 bd : basal direct

37 CEAAR: Caryopsis Endosperm Assimilate Acquisition Route

38 DPA: Days Post Anthesis

39 IPC: Inner Pericarp Cells

40 vc: ventral circuituous

41 vd: ventral direct

42

43 **Introduction**

44 Cereals are major source of food and feed for humans and their livestock. The value of cereals lies
45 in the dry storage capacity of their endosperm. An endosperm is a sink tissue, therefore assimilates
46 stored in the endosperm originate from source tissues in other parts of the plant. During grain
47 filling, assimilates are translocated from source tissues towards the endosperm through the vascular
48 bundle. Because of the absence of vascular continuity between maternal source tissues and filial
49 sink tissues, assimilates are unloaded from the phloem and traverse post-phloem transfer cells on
50 their journey to the endosperm. Thus, the post-phloem transport pathway serves as a bridge
51 connecting maternal supply to filial sink of cereal caryopsis. Based on studies of assimilate
52 movement into developing filial tissues of cereals like rice, maize, sorghum, barley and wheat, three
53 models for post-phloem transport pathway into caryopses endosperms can be deduced. These
54 models, which we collectively termed Caryopsis Endosperm Assimilate Acquisition Route
55 (CEAAR) models are; basal direct (bd), ventral circuituous (vc), ventral direct (vd) and (Fig. 1).
56 Barley and wheat represent the first model; vd-CEAAR. In these species, assimilates are also
57 delivered by a ventrally located grain vascular tissue that run the length of the grain. On exit from
58 the phloem, assimilates symplastically cross chalazal cells, nucellar projection cell sand accumulate
59 temporally in an apoplastic space called the endosperm cavity. Specialized endosperm transfer cells
60 (also called modified aleurone cells) handles the importation of assimilates from the endosperm
61 cavity into the endosperm (Fig. 1a) (Cochrane, 1985;Cochrane and Duffus, 1980; Donovan et al.,
62 1983; Frazier and Appalanaidu, 1965; H. L.Wang, C. E. Offler, et al., 1995; H. L. Wang, J. W.
63 Patrick, et al., 1995; Zheng and Wang, 2011).

64

65 An example of vc-CEAAR is found in rice, where assimilates are delivered by the ovular vascular
66 tissue that runs the entire length of the ventral surface of developing rice grains.

67 Assimilates symplastically traverse the chalazal zone, a remnant of nucellar and move into nucellar
68 epidermis cells. Within the nucellar epidermis, they move circumferentially around the developing
69 endosperm and eventually cross the plasma membrane of the nucellar epidermis cell into an
70 apoplastic space adjoining the aleurone cells. From this space they are imported into aleurone cells
71 and further into starchy endosperm cells (Fig. 1b) (Ellis and Chaffey, 1987; Krishnan and
72 Dayanandan, 2003; Oparka and Gates, 1981, 1982; Wu et al., 2016). The third model, bd-CEAAR,
73 is seen in maize and sorghum. Here the vascular trace ends at the base of the grain. Assimilates

74 headed for storage in the endosperm are released from the phloem sieve tubes, from there they cross
75 the chalazal strip and remnant nucellar cells. In sorghum and some varieties of maize, assimilates
76 accumulate in the placental sac which serves as a transient sink. Basal Endosperm transfer layer
77 (BETL) cells are responsible for transport of assimilates from the placental sac into the developing
78 endosperm (Fig. 1c) (Felker and Shannon, 1980; Maness and McBee, 1986; Thorne, 1985; Zheng et
79 al., 2015).

80

81 The importance of post-phloem assimilate transfer cells for proper caryopses development is easily
82 manifest when there is perturbation of normal gene regulation and expression in the transfer cells.
83 For example, maize *MINIATURE1* (*MN1*) and rice *GRAIN INCOMPLETE FILLING* (*GIF1*) loci
84 encodes cell wall invertases that are expressed in the transfer cells of maize and rice grains
85 respectively. Null mutation of *MN1* or mis-regulation of *GIF1* results in smaller grains compared to
86 wild type (Cheng et al., 1996; Miller and Chourey, 1992; Wang et al., 2008). Similarly in barley,
87 mature grains of shrunken endosperm genetic (*seg*); *seg1*, *seg3*, *seg6* and *seg7* mutants are shrunken
88 because post-phloem transfer cells collapse early compared to wild type, leading to premature
89 cessation of grain filling (Bosnes et al., 1992; Felker et al., 1985, 1984, 1983). Furthermore, maize
90 *ZmSWEET4c* and its rice ortholog *OsSWEET4* are hexose transporters expressed in post-phloem
91 transfer cells. Their loss of function mutation results in incomplete grain filling (Sosso et al., 2015).
92 In view of the importance of the expression of *GIF1*, *OsSWEET4* and *ZmSWEET4c* in the post-
93 phloem transfer cells of rice and maize respectively, for proper grain filling, they no doubt
94 contribute to large grain trait of these cereals and are therefore postulated to have been recruited
95 during the domestication of these cereals (Doebley et al., 2006; Sosso et al., 2015; Wang et al.,
96 2008).

97

98 *Brachypodium distachyon* (subsequently, *Brachypodium*) on the other hand is a wild grass that
99 recently became a model system for temperate cereals. *Brachypodium* grains are comparable to
100 barley and wheat in length, but are narrower in width and shallower in depth (Hands and Drea,
101 2012). Although, median transverse section profiles of *Brachypodium* grains are generally identical
102 to barley, wheat and oat sections, *Brachypodium* grains have reduced nucellar projection and
103 persistent nucellar epidermis (Kosina and Tomaszewska, 2016; Opanowicz et al., 2011). Notably,
104 modified aleurone, critical for assimilate import into the endosperm of barley and wheat is absent in
105 *Brachypodium* grains. This attribute suggests that the final step of assimilate import into
106 *Brachypodium* endosperm employs a different route compared to wheat and barley. Hence, we
107 speculated that assimilate movement into *Brachypodium* endosperm follows the vc-CEAAR model

108 as found in rice (Hands et al., 2012). In this study, we used fluorescent dyes; 5-(6)-6
109 carboxyfluorescein diacetate (CFDA) and Lucifer Yellow (LW) to trace the path of assimilate
110 movement into Brachypodium endosperm.

111

112 We confirm that the route of assimilate import into Brachypodium endosperm is similar to rice and
113 can be classified as vc-CEAAR. In addition, we report detailed ultrastructural study of caryopsis
114 post-phloem transfer cells of Brachypodium. Our results highlight the anatomical basis for the route
115 of assimilate transport into Brachypodium endosperm. Structural similarities and differences
116 between the caryopses post-phloem transfer cells of Brachypodium and major cereals relevant to
117 assimilate import into the endosperm are discussed.

118

119 **Materials and Methods**

120 *Growth of Brachypodium plants*

121 Brachypodium (Bd 21) Grains, were imbibed on moist filter paper in a Petri dish and left at 5°C for
122 two days to vernalize. They were transferred to room temperature (about 25-27°C) and left to
123 germinate. After 7 days, the most virile seedlings were transferred to 9:1 Levington M2 Pot and
124 Bedding Compost: Levington Fine Vermiculite mix (dejex.co.uk), in Vacapot™ 15 on plastic seed
125 trays (www.plantcell.co.uk). They were grown in the greenhouse at 16hr daylight and 25°C
126 temperature. The plants were regularly watered manually. Flowering spikes were tagged at anthesis
127 and sampled at 5 days interval after anthesis until 30 days post anthesis (DPA).

128

129

130 *Fluorescence tracer experiments*

131 Fluorescence dyes used are symplastic tracer; 0.01% 5-(6)-6-carboxyfluorescein diacetate
132 (CFDA; Sigma) and apoplastic tracer; 1% Lucifer Yellow (LY; Sigma). Sterile distilled water
133 served as control. Brachypodium grains were carefully detached from their rachis at 20 DPA and
134 their lemma removed under a dissecting microscope. About 20 grains were incubated in 1 ml
135 solution of either fluorescent dyes or water in 1.5 ml Eppendorf tubes at room temperature.
136 Five grains were sampled from each treatment at 15, 30, 45 and 60min. This was followed by a
137 vigorous rinse in 1 ml distilled water three times before the grains were transferred to 0.5 ml 50%
138 glycerol. Free hand 80 – 150 µm transverse sections spanning the length of the grains were made
139 with clean razor blades. The sections were mounted on 50% glycerol covered with cover slips and
140 the edges sealed with nail varnish. Imaging was done with Nikon ECLIPSE 80i fluorescence
141 microscope (Nikon, Japan), having an LED-based excitation source (CoolLED, presicExcite), using

142 Nikon Plan Fluor 10x /0.30 DIC L/N1 objective lens. Fluorescence images were captured with a
143 DS-QiMc cooled CCD camera (Nikon, Japan). Images were previewed, captured and saved using
144 NIS-Elements Basic Research v3.0 software (Nikon, Japan) in JPEG2000 format.

145

146 *Brachypodium grain processing for light and transmission electron microscopy*

147 Individual Brachypodium florets were tagged at anthesis and developing grains were sampled at
148 five days interval until 30 days after anthesis (DPA), six developmental stages in total. At each
149 interval, five grains were collected from different florets. 1 mm section was cut from the mid grain
150 region of each grain, using a dissecting microscope. Sections were fixed in 2.5% glutaraldehyde in
151 0.1M sodium Cacodylate buffer pH 7.4, for 3 days at 4°C with constant gentle agitation and then
152 washed in 0.1M Sodium Cacodylate buffer. After further fixation in 1% aqueous osmium tetroxide
153 and dehydration in series of increasing ethanol concentrations followed by propylene oxide, the
154 seed sections were embedded in Spurr's hard resin and polymerised for 16 hours at 60°C.

155

156 *Light microscopy*

157 Grain sections for light microscopy were cut 400nm thick, stained with 0.01% toluidine blue,
158 mounted in resin, then viewed and photographed with GX L3200B compound microscope
159 (gtvision.co.uk) equipped with a CMEX-5000 USB2 Microscope camera and ImageFocus 4
160 software (euromex.com). Images were stored as TIFF files and annotated with Adobe
161 Illustrator.

162

163 *Electron microscopy*

164 70nm thick sections for transmission electron microscopy were cut using a Reichert Ultracut
165 E ultra microtome. The sections were collected onto copper mesh grids, and stained with
166 2% aqueous uranyl acetate for 30 minutes followed by 5 minutes in lead citrate. Sections were
167 viewed on a JEOL JEM-1400 TEM (www.jeolusa.com) with an accelerating voltage of
168 100kV. Digital images were collected with a Megaview III digital camera with iTEM software
169 (emsis.eu) as TIFF files.

170

171 **Results**

172 *Cellular structure of assimilate transfer route in Brachypodium grains*

173 *Vascular bundle*

174 Groups of sieve element – companion cells (se – cc) complex was observed on the ventral

175 (adaxial) vascular bundle on all the grains sampled at all stages. The number of se – cc complex
176 varied between grains at the same developmental stage but generally increased as the grain
177 develops. Characteristic of monocots, the se – cc complexes were irregularly scattered between
178 vascular parenchyma cells (Fig. 2b, d-g), except at 10 DPA when they seemingly formed a semi-
179 circle facing towards the pigment strand (Fig. 2a, c). Mixtures of mature (empty lumen) and
180 immature (lumen with remnants of cytoplasm) sieve elements cells were observed in all sample
181 stages (Fig. 3a). The accompanying companion cells were not always easily identified. They were
182 smaller and usually had denser cytoplasm compared to vascular parenchyma cells (Fig. 3a).
183 Plasmodesmata connections were observed between sieve elements and their companion cells, as
184 well as between sieve elements and vascular parenchyma cells. Similarly, there were
185 plasmodesmata connections between companion cells and vascular parenchyma cells. Remarkably,
186 we could not identify any xylem elements in sections from all the stages.

187

188 *Pigment strand*

189 The pigment strand is located inwards of the vascular bundle toward the endosperm. The pigment
190 strand is remarkable for cells that accumulate dark deposits as the grain develops. At
191 5 DPA, the cells of the pigment strand can be distinguished from those of vascular parenchyma
192 bundles by their elongate shape and generally denser cytoplasm. Dark deposits were detected on a
193 few of the cells in the pigment strand at 5DPA. They appeared to first accumulate in small amount,
194 in a subcellular organelle, possibly the vacuole. The organelle then enlarges, with the already
195 accumulated deposit forming a continuous ring bordering the membrane of the organelle. The rest
196 of the cytoplasm is pushed against the cell wall as the organelle expands. The initial clear space
197 created within the organelle by its enlargement is eventually filled with the dark deposit as the grain
198 matures (Fig. 2a-g; Fig. 3b-d). The number of pigment strand cells filled with dark deposit
199 increased at subsequent sampling stages. Note that even at 30 DPA, there were still pigment strand
200 cells that had not accumulated dark deposits. Abundant plasmodesmata connections were observed
201 between adjacent pigment strand cells (whether filled with dark deposit or not), between pigment
202 strand cells and vascular parenchyma cells, and, between pigment strand cells and nucellar
203 projection cells (Fig. 3).

204

205 Four layers of different cell types flank the pigment strand on both sides and are continuous round
206 the developing endosperm (Fig. 2a-b). They are tube cells (CC), outer integument
207 (OI), inner integument (II) and nucellar epidermis (NE), in that order from the outer surface.
208 For brevity we will refer to them as inner pericarp cells (IPC).

209

210 Tube cells are bordered on the outside by mesocarp cells and on the inside by the outer integument.
211 They are easily distinguished from the mesocarp cells by their lack of chloroplasts, circular shape
212 and sparse cytoplasm. Tube cells had thin cell walls in all the samples examined and enlarge as the
213 grain develops till around 20 DPA. They subsequently appeared shrunk in size and separate from
214 one another by 30 DPA.

215

216 The outer integument cells have sparse cytoplasm and enlarge as the grain develops till about
217 20 DPA. The cell walls of outer integument cells adjacent to tube cells are already cutinized at 5
218 DPA and progressively become heavily cutinized as the grain matures (Fig. 2b-g). The inner cell
219 walls abutting the inner integument also become cutinized to a lesser degree as the grain develops.
220 From 25 DPA, outer integument cells collapse and appear as one layer of cutin. The collapse of the
221 outer integument cells starts from the dorsal grain surface and proceeds to the ventral surface.

222

223 Inner integument cells lie between the outer integument and nucellar epidermis. Inner integument
224 cells are filled with dark deposits in the manner already described for pigment strand cells. The
225 deposits have been identified in barley as tannins (Briggs, 1974; Felker et al., 1984).

226

227 Nucellar epidermis cells are the largest of the cell types in a developing Brachypodium grain at
228 5 DPA (Fig. 2a). The lateral nucellar epidermis cells are usually the largest (Opanowicz et al.,
229 2011). Nucellar epidermis cells reach peak size at about 15 DPA. Subsequently, they gradually
230 become smaller, possibly as a result of pressure from the expanding endosperm. Adjacent nucellar
231 epidermis cells are separated by thin cell walls with prominent plasmodesmata.

232 However, nucellar epidermis cell walls in contact with endosperm cells and inner integument cells
233 are greatly thickened (Fig. 3e). Gullion et al, (2012), detected (1-3) (1-4)- β -D glucan in the inner
234 and outer cell walls of nucellar epidermis cells in 7 DPA developing Brachypodium grains. The
235 cytoplasm of nucellar epidermis cells appeared vacuolated at early stages of development. At later
236 stages of development the cells were found filled with electron lucent cellulosic material, previously
237 identified as (1-3) (1-4)- β -D glucan (Guillon et al., 2012). A prominent middle lamella was
238 observed between nucellar epidermis cells and inner integument cells (Fig. 3e).

239

240 There are plasmodesmata connections between adjacent pigment strand cells and cells of these four
241 cell types on both flanks. Plasmodesmata connections were not observed between the different
242 types of cells that make up the IPC.

243

244 *Nucellar projection*

245 Nucellar projection cells adjoins the pigment strand inwards towards the endosperm. Brachypodium
246 nucellar projection cells can be distinguished into two types; (a) smaller and circular type close to
247 the pigment strand that have dense cytoplasm, (b) larger and elongate type close to the endosperm
248 that have sparse cytoplasm (Fig. 2). The cell walls of nucellar projection cells greatly thicken as the
249 grain matures, especially the elongate nucellar cells close to the endosperm (Fig. 3f). A progressive
250 increase in the cell wall thickening of nucellar projection cells from the pigment strand to the
251 endosperm was observed. Signs of lysing of nucellar projection cells close to the endosperm were
252 observed on grain sections from 10 – 30 DPA.

253 Numerous plasmodesmata connections were observed between adjacent nucellar projection cells.

254

255 *Endosperm cavity*

256 Endosperm cavity was not observed on Brachypodium grains sampled at 5 and 10 DPA. At
257 15 DPA (Fig. 2d), endosperm cavity was observed between the endosperms and nucellar projection.
258 The cavity was still present at 20 DPA (Fig. 2e), though occupying a lesser area compared to 15
259 DPA. By 25 DPA, the cavity has been completely occluded by the expanding endosperm (Fig. 2f).

260

261 *Assimilate transfer pathway into developing Brachypodium grains*

262 Delineation of assimilate transport pathway into developing Brachypodium grains was investigated
263 using fluorescent dyes; symplastic tracer; 5-(6)-6-carboxyfluorescein diacetate (CFDA; Sigma) and
264 apoplastic tracer; 1% Lucifer Yellow (LY; Sigma). The grains were incubated in the dye solutions
265 for different lengths of time and the localization of the dyes were confirmed using fluorescence
266 microscopy.

267

268 CFDA was readily observed on transverse free hand sections of the Brachypodium grains that had
269 been incubated in the dye for 15min. CFDA fluorescence was distinctly observed on the vascular
270 bundle, pigment strand cells, nucellar projection cell and round the grain in nucellar epidermis cells
271 (Fig. 4). Similar, results were obtained on grains incubated in the dye for 30, 45 and 60min. As the
272 period of incubation increased, dye fluorescence increased centripetally in the endosperm. This
273 suggests that materials travel circumferentially around the grain and at some point cross into
274 endosperm cells. So the longer the grains were incubated, the more CFDA is centripetally
275 accumulated, evidenced by intense fluorescence in the endosperm of grains sectioned after 60min
276 incubation in CFDA (data not shown).

277

278 Fluorescent signals were not detected in sections of Brachypodium grains incubated in Lucifer
279 Yellow for any of the period of time used in this experiment (data not shown). Since Lucifer yellow
280 is an apoplastic dye, this suggests that assimilate movement into Brachypodium endosperm may be
281 largely symplastic.

282

283 **Discussion**

284 The succession of cell types in the post-phloem assimilate delivery pathway of Brachypodium
285 represent a combination of features of such pathways reported in wheat, barley and rice. A ventral
286 vascular bundle that spans the length of the caryopsis is a common feature in these three species
287 (Thorne, 1985). The grain vascular bundle is connected to the rachilla and serves as route of water
288 and assimilate transport from the rest of the plant into developing caryopsis (Frazier and
289 Appalanaidu, 1965; Lingle and Chevalier, 1985). Our observation of the formation of semi-circle by
290 the phloem of the vascular bundle of Brachypodium grains at 10 DPA (Fig. 2a, c) corresponds to
291 observation of a phloem arc in rice caryopsis at 12 DPA (Oparka and Gates, 1981). The occurrence
292 of immature sieve elements containing little cytoplasm alongside mature sieve elements with empty
293 lumen has also been reported in rice (Oparka and Gates, 1981). Since the vascular bundle continue
294 to differentiate as the grain develops, the immature sieve elements observed may be newly
295 differentiated ones. Plasmodesmata connection among and between cells of the vascular bundle of
296 Brachypodium grains suggest symplastic exchange of water and assimilates between these cells.
297 This is similar to observations in rice and wheat (Oparka and Gates, 1981; H. L. Wang, C. E. Offler,
298 et al., 1995). Also, Plasmodesmata connection between cells of the vascular bundle and surrounding
299 parenchyma cells is consistent with observations in wheat (H. L. Wang, C. E. Offler, et al., 1995).
300 This arrangement of cells suggest that assimilates move vertically up from the base of the grain
301 through the vascular bundle and are discharged horizontally into the parenchyma cells along the
302 way.

303

304 Sucrose is the main sugar transported in grasses (Thorne, 1985; van Bel and Hess, 2008).
305 Sucrose is cleaved to hexoses on exit from the vascular bundle in maize and sorghum by vacuolar
306 and cell wall invertases (Bihmidine et al., 2013; Felker and Shannon, 1980; Maness and McBee,
307 1986; Porter et al., 1985). In wheat and barley, whether or not sucrose is cleaved after it is unloaded
308 from the vascular bundle remains a debate (Thorne, 1985). In any case, accumulation of glucose in
309 wheat endosperm cavity sap coupled with 80% reduction of sucrose concentration compared to
310 sieve tube sap strongly suggests that sucrose is cleaved in the post-phloem transfer cells of wheat

311 (Fisher and Gifford, 1986). Whether or not sucrose is transformed in the post-phloem pathway of
312 Brachypodium is an interesting research question. However, the dense cytoplasm of the vascular
313 bundle and parenchyma cells suggest they are not just passive channels of for assimilate movement.
314 The abundance of mitochondria in these cells suggest the occurrence of energy demanding
315 processes. This sharply contrasts with surrounding mesocarp cells which gradually lose their
316 cytoplasm as the grain develops, and but for chloroplasts, appear empty at 30 DPA.

317

318 The presence of pigment strand have been reported in barley rice and wheat (Felker et al., 1984;
319 Oparka and Gates, 1982; H. L. Wang, C. E. Offler, et al., 1995). While the pigment strand cells of
320 rice grain accumulate lipid deposits, those of wheat and barley accumulate phenolic deposits (Felker
321 et al., 1984; Oparka and Gates, 1982). The pigment strand in Brachypodium is strikingly similar to
322 barley in the extent it gets filled with dark deposits (Lingle and Chevalier, 1985). Dark deposits in
323 Brachypodium pigment strand cells were visible at 5 DPA whereas they appears at about 12 DPA in
324 barley (Felker et al., 1984; Lingle and Chevalier, 1985), suggesting early accumulation of dark
325 deposits in Brachypodium. The accumulation of deposits in pigment strand cells was initially
326 thought to limit assimilate transport towards the endosperm during wheat grain development (Zee
327 and O'brien, 1970). Subsequent reports failed to confirm this view, but rather suggested that
328 assimilate transport is restricted to the symplast at the pigment strand (Lingle and Chevalier, 1985;
329 Oparka and Gates, 1982). On the basis of comparative anatomy, we speculate that assimilate
330 movement into developing Brachypodium grains may not be limited by the accumulation of dark
331 deposits in its pigment strand cells. Whether assimilate transport is restricted to the symplast at the
332 pigment strand of Brachypodium cannot be firmly confirmed from our results. However, the high
333 frequency of plasmodesmata connection between pigment strand cells and vascular parenchyma
334 cells suggest an increased transportation capacity that may compensate for loss of apoplastic
335 transport between the vascular parenchyma cells and the pigment strand cells.

336

337 Plasmodesmata connection between pigment strand cells and IPC, namely; tube cells, outer
338 integument, inner integument and nucellar epidermis, suggest that assimilate supply to these cells
339 may rely significantly on pigment strand cells. These cells are already well differentiated at 5 DPA.
340 Our observations suggest little or no cell division in these four flanking cell types as the grain
341 develops. They greatly enlarge and further differentiate by accumulation and synthesis of materials
342 as during grain development. Since they lack chlorophyll, the materials they need are mostly likely
343 supplied through the pigment strands. Thus, suggesting that Brachypodium pigment strand cells
344 may serve as a hub for assimilate distribution to different types of cells. This therefore raises the

345 question; to what extent does assimilate supply to other grain cell types deprive Brachypodium
346 endosperm resources for starch synthesis? We plan to answer this question in a future experiment.
347

348 Based on cell morphology, we identified only two types of nucellar projection cells in
349 Brachypodium, whereas three and four types of nucellar projection cells were identified in barley
350 and wheat respectively (Thiel et al., 2008; Wang et al., 1994). However, as in barley and wheat, the
351 nucellar projection cells closest to the pigment strand were the least differentiated and those closest
352 to the endosperm had massive cell walls. Compared to wheat and barley nucellar projection cells do
353 not undergo extensive autolysis as the grain develops in Brachypodium.

354 The limited lysing of nucellar projection cells (Fig. 2d-e) creates a transient cavity that is smaller
355 but similar to the endosperm cavity of wheat and barley. The endosperm cavity serves as a
356 temporary apoplastic sink for assimilates (H. L. Wang, C. E. Offler, et al., 1995; H. L. Wang, J. W.
357 Patrick, et al., 1995). The presence of endosperm cavity contribute to grain shape in cereals (Hands
358 et al., 2012). Thus, the transient endosperm cavity contribute to the narrow crease in a mature
359 Brachypodium grains (Hands and Drea, 2012).

360

361 Whereas nucellar cells in barley, maize, rice, sorghum and wheat usually undergo programmed cell
362 death (PCD) and lyse after fertilization (Radchuk and Borisjuk, 2014), Brachypodium nucellar cells
363 are slow to die and the nucellar epidermis remain prominent and persistent throughout grain
364 development (Solomon and Drea, unpubl. data). Remarkably, the cell walls of nucellar projection
365 cells in developing Brachypodium grains become thick, but lack wall ingrowths as found in barley
366 and wheat (Cochrane and Duffus, 1980; Wang et al., 1994). Wall ingrowths in nucellar projection
367 cells and other types of transfer cells, potentially increase plasma membrane surface area for rapid
368 assimilate transport (Offler et al., 2003; H. L. Wang, C. E. Offler, et al., 1995).

369

370 It is tempting to speculate that the lack of wall ingrowths in nucellar projection cells of
371 Brachypodium grains may contribute to lower post-phloem assimilate transport capacity compared
372 to wheat and barley. This speculation is plausible considering that assimilate delivery to developing
373 barley and wheat endosperms relies only on nucellar projection cells for passage of assimilates from
374 the pigment strand into the endosperm cavity. Hence the need for the increased surface area for
375 rapid assimilate movement. Whereas in Brachypodium, assimilates are also transported through
376 nucellar epidermis (Fig. 4), in addition to the nucellar projection. This additional channel for
377 assimilate movement probably means that less assimilate pass through Brachypodium nucellar
378 projection cells compared to wheat and barley. However, numerous plasmodesmata connection

379 between cells of Brachypodium nucellar projection cells (despite thickened cell walls) suggest a
380 capacity for rapid assimilate movement across these cells. The thick walls of Brachypodium
381 nucellar projection cells may also provide apoplastic route of assimilate and water movement
382 towards the endosperm as reported in wheat (H. L. Wang, C. E. Offler, et al., 1995).

383

384 Assimilate movement into Brachypodium endosperm is identical to rice where the main supply
385 route is circumferentially via the nucellar epidermis (Fig. 1b). In rice, several sucrose transport
386 genes have been shown to be expressed along the post-phloem assimilate delivery pathway to
387 developing grains (Bai et al., 2016; Furbank et al., 2001; Ma et al., 2017). While some of the genes
388 have active roles in sucrose export from the nucellar epidermis into the maternal/filial apoplast,
389 others have been linked with assimilate import into aleurone cells (Ma et al., 2017). Mutation of
390 sucrose transport genes and/or their regulators negatively affects grain filling and lead to
391 abnormally shaped rice grains (Bai et al., 2016; Ma et al., 2017; Wu et al., 2018). Though sucrose
392 transport genes are conserved in Brachypodium (Braun and Slewinski, 2009), their role in
393 assimilate transport and grain filling is yet to be reported. Nevertheless, a major structural
394 difference is that in rice, nucellar epidermis cells collapse during grain development while in
395 Brachypodium they persist till grain maturity. Based on earlier histological studies, it was suggested
396 that mechanical compression of rice nucellar epidermis by expanding endosperm prevents further
397 flow of assimilates and terminate grain filling (Ellis and Chaffey, 1987; Ellis et al., 1987). However,
398 recent findings have demonstrated programmed cell death (PCD) in nucellar tissues of developing
399 rice grains (Yang et al., 2012; Yin and Xue, 2012). It has also been shown that perturbation of genes
400 involved in PCD of nucellar tissues adversely affects grain filling and lead to abnormally shaped
401 grains (Nayar et al., 2013; Yang et al., 2012; Yin and Xue, 2012). Furthermore, PCD of nucellar
402 tissues is known to be generally necessary for normal grain development in cereals (Domínguez and
403 Cejudo, 2014; Lu and Magnani 2018). It is therefore remarkable that normal grain development and
404 filling in Brachypodium does not require disintegration of nucellar epidermis cells. We previously
405 showed that nucellar epidermis cells are dead in mature Brachypodium grain (Hands et al., 2012).
406 However, there is no data yet on when and how its death affects grain development and filling. An
407 additional feature of Brachypodium nucellar epidermis cells is accumulation (1-3) (1-4)- β -D glucan
408 as the grain develops (Guillon et al., 2012). It is not clear if and how accumulation of (1-3) (1-4)- β -
409 D glucan in nucellar epidermis cells affect assimilate transport through these cells. It is possible that
410 (1-3) (1-4)- β -D glucan accumulation in the nucellar epidermis cells deprive the endosperm of
411 assimilates and decrease the rate of assimilate transport.

412

413 **Conclusion**

414 The fine structure and post-phloem assimilate transport into developing grains of *Brachypodium*
415 reflects the species phylogenetic position between Ehrhartoideae and Pooideae. *Brachypodium*
416 post-phloem assimilate delivery pathway is structurally similar to wheat and barley save for the
417 absence of modified aleurone. Its assimilate delivery strategy on the other hand is identical rice.
418 These combination of temperate anatomy with tropical physiology marks *Brachypodium* as an
419 excellent model to understand the evolution of specialised assimilate transfer cells (modified
420 aleurone) for efficient assimilate acquisition in temperate cereal grains. Such knowledge can be
421 exploited in domestication of new crop species.

422

423 **Acknowledgements**

424 We are grateful to Natalie Allcock and Anna Straatman-Iwanowska for assistance with grain
425 sectioning and electron microscopy. CUS is a PhD student funded by Tertiary Education Trust
426 Fund, Nigeria.

427

428

429

430

431

432

433

434

435

436

437

438

439

440

441

442

443

444

445

446

447

448

449

450

451

References

Bai, A.-N., Lu, X.-D., Li, D.-Q., Liu, J.-X., Liu, C.-M., 2016. NF-YB1-regulated expression of sucrose transporters in aleurone facilitates sugar loading to rice endosperm. *Cell Research* 26, 384–388. <https://doi.org/10.1038/cr.2015.116>

Bihmidine, S., Hunter, C.T.I., Johns, C.E., Koch, K.E., Braun, D.M., 2013. Regulation of assimilate import into sink organs: Update on molecular drivers of sink strength. *Frontiers in Plant Science* 4. <https://doi.org/10.3389/fpls.2013.00177>

Bosnes, M., Weideman, F., Olsen, O.-A., 1992. Endosperm differentiation in barley wild- type and sex mutants. *The Plant Journal* 2, 661–674. <https://doi.org/10.1111/j.1365-313X.1992.tb00135.x>

Braun, D.M., Slewinski, T.L., 2009. Genetic Control of Carbon Partitioning in Grasses: Roles of Sucrose Transporters and Tie-dyed Loci in Phloem Loading. *Plant Physiology* 149, 71–81. <https://doi.org/10.1104/pp.108.129049>

Cheng, W.H., Taliercio, E.W., Chourey, P.S., 1996. The Miniature1 Seed Locus of Maize Encodes a Cell Wall Invertase Required for Normal Development of Endosperm and Maternal Cells in the Pedicel. *The Plant Cell* 8, 971–983. <https://doi.org/10.1105/tpc.8.6.971>

Cochrane, M.P., 1985. Assimilate Uptake and Water Loss in Maturing Barley Grains. *Journal of Experimental Botany* 36, 770–782. <https://doi.org/10.1093/jxb/36.5.770>

Cochrane, M.P., Duffus, C.M., 1980. The nucellar projection and modified aleurone in the crease region of developing caryopses of barley (*Hordeum vulgare* L. var. *Distichum*). *Protoplasma* 103, 361–375. <https://doi.org/10.1007/BF01276962>

Doebley, J.F., Gaut, B.S., Smith, B.D., 2006. The Molecular Genetics of Crop Domestication. *Cell* 127, 1309–1321. <https://doi.org/10.1016/j.cell.2006.12.006>

Domínguez, F., Cejudo, F.J., 2014. Programmed cell death (PCD): An essential process of cereal seed development and germination. *Frontiers in Plant Science* 5. <https://doi.org/10.3389/fpls.2014.00366>

Donovan, G.R., Jenner, C.F., Lee, J.W., Martin, P., 1983. Longitudinal Transport of Sucrose and Amino Acids in the Wheat Grain. *Functional Plant Biology* 10, 31–42. <https://doi.org/10.1071/pp9830031>

Ellis, J.R., Chaffey, N.J., 1987. Structural Differentiation of the Nucellar Epidermis in the Caryopsis of Rice (*Oryza sativa*). *Annals of Botany* 60, 671–675. <https://doi.org/10.1093/oxfordjournals.aob.a087498>

Ellis, J.R., Gates, P.J., Boulter, D., 1987. Storage-protein Deposition in the Developing Rice Caryopsis in Relation to the Transport Tissues. *Annals of Botany* 60, 663–670. <https://doi.org/10.1093/oxfordjournals.aob.a087497>

Felker, F.C., Peterson, D.M., Nelson, O.E., 1985. Anatomy of Immature Grains of Eight Maternal Effect Shrunken Endosperm Barley Mutants. *American Journal of Botany* 72, 248–256. <https://doi.org/10.1002/j.1537-2197.1985.tb08289.x>

Felker, F.C., Peterson, D.M., Nelson, O.E., 1984. Development of tannin vacuoles in chalaza and seed coat of barley in relation to early chalazal necrosis in the *seg1* mutant. *Planta* 161, 540–549. <https://doi.org/10.1007/BF00407087>

Felker, F.C., Peterson, D.M., Nelson, O.E., 1983. Growth Characteristics, Grain Filling, and Assimilate Transport in a Shrunk Endosperm Mutant of Barley. *Plant Physiology* 72, 679–684. <https://doi.org/10.1104/pp.72.3.679>

Felker, F.C., Shannon, J.C., 1980. Movement of ¹⁴C-labeled Assimilates into Kernels of *Zea mays* L: III. AN ANATOMICAL EXAMINATION AND MICROAUTORADIOGRAPHIC STUDY OF ASSIMILATE TRANSFER. *Plant Physiology* 65, 864–870. <https://doi.org/10.1104/pp.65.5.864>

Fisher, D.B., Gifford, R.M., 1986. Accumulation and Conversion of Sugars by Developing Wheat Grains: VI. Gradients Along the Transport Pathway from the Peduncle to the Endosperm Cavity during Grain Filling. *Plant Physiology* 82, 1024–1030. <https://doi.org/10.1104/pp.82.4.1024>

Frazier, J.C., Appalanaidu, B., 1965. The Wheat Grain during Development with Reference to Nature, Location, and Role of Its Translocatory Tissues. *American Journal of Botany* 52, 193–198. <https://doi.org/10.1002/j.1537-2197.1965.tb06775.x>

Furbank, R.T., Scofield, G.N., Hirose, T., Wang, X.-D., Patrick, J.W., Offler, C.E., 2001. Cellular localisation and function of a sucrose transporter OsSUT1 in developing rice grains. *Functional Plant Biology* 28, 1187–1196. <https://doi.org/10.1071/pp01111>

Guillon, F., Larré, C., Petipas, F., Berger, A., Moussawi, J., Rogniaux, H., Santoni, A., Saulnier, L., Jamme, F., Miquel, M., Lepiniec, L., Dubreucq, B., 2012. A comprehensive overview of grain development in *Brachypodium distachyon* variety Bd21. *Journal of Experimental Botany* 63, 739–755. <https://doi.org/10.1093/jxb/err298>

Hands, P., Drea, S., 2012. A comparative view of grain development in *Brachypodium distachyon*. *Journal of Cereal Science, Cereal Grain Development: Molecular Mechanisms and Impacts on Grain Composition and Functionality* 56, 2–8. <https://doi.org/10.1016/j.jcs.2011.12.010>

Hands, P., Kourmpetli, S., Sharples, D., Harris, R.G., Drea, S., 2012. Analysis of grain characters in temperate grasses reveals distinctive patterns of endosperm organization associated with grain shape. *Journal of Experimental Botany* 63, 6253–6266. <https://doi.org/10.1093/jxb/ers281>

Kosina, R., Tomaszewska, P., 2016. Variability of breeding system, caryopsis microstructure and germination in annual and perennial species of the genus *Brachypodium* P. Beauv. *Genetic Resources and Crop Evolution* 63, 1003–1021. <https://doi.org/10.1007/s10722-015-0297-4>

Krishnan, S., Dayanandan, P., 2003. Structural and histochemical studies on grain-filling in the caryopsis of rice (*Oryza sativa* L.). *Journal of Biosciences* 28, 455–469. <https://doi.org/10.1007/BF02705120>

Lingle, S.E., Chevalier, P., 1985. Development of the Vascular Tissue of the Wheat and Barley Caryopsis as Related to the Rate and Duration of Grain Filling 1. *Crop Science* 25, 123–128. <https://doi.org/10.2135/cropsci1985.0011183X002500010031x>

Lu, J., Magnani, E., 2018. Seed tissue and nutrient partitioning, a case for the nucellus. *Plant Reproduction* 31, 309–317. <https://doi.org/10.1007/s00497-018-0338-1>

Ma, L., Zhang, D., Miao, Q., Yang, J., Xuan, Y., Hu, Y., 2017. Essential Role of Sugar Transporter OsSWEET11 during the Early Stage of Rice Grain Filling. *Plant and Cell Physiology* 58, 863–873. <https://doi.org/10.1093/pcp/pcx040>

Maness, N.O., McBee, G.G., 1986. Role of Placental Sac in Endosperm Carbohydrate Import in Sorghum Caryopses 1. *Crop Science* 26, 1201–1207. <https://doi.org/10.2135/cropsci1986.0011183X002600060026x>

Miller, M.E., Chourey, P.S., 1992. The Maize Invertase-Deficient miniature-1 Seed Mutation Is Associated with Aberrant Pedicel and Endosperm Development. *The Plant Cell* 4, 297–305. <https://doi.org/10.1105/tpc.4.3.297>

Nayar, S., Sharma, R., Tyagi, A.K., Kapoor, S., 2013. Functional delineation of rice MADS29 reveals its role in embryo and endosperm development by affecting hormone homeostasis. *Journal of Experimental Botany* 64, 4239–4253. <https://doi.org/10.1093/jxb/ert231>

Offler, C.E., McCurdy, D.W., Patrick, J.W., Talbot, M.J., 2003. Transfer Cells: Cells Specialized for a Special Purpose. *Annual Review of Plant Biology* 54, 431–454. <https://doi.org/10.1146/annurev.arplant.54.031902.134812>

Opanowicz, M., Hands, P., Betts, D., Parker, M.L., Toole, G.A., Mills, E.N.C., Doonan, J.H., Drea, S., 2011. Endosperm development in *Brachypodium distachyon*. *Journal of Experimental Botany* 62, 735–748. <https://doi.org/10.1093/jxb/erq309>

Oparka, K.J., Gates, P., 1981. Transport of assimilates in the developing caryopsis of rice (*Oryza sativa* L.). *Planta* 151, 561–573. <https://doi.org/10.1007/BF00387436>

Oparka, K.J., Gates, P.J., 1982. Ultrastructure of the developing pigment strand of rice (*Oryza sativa* L.) in relation to its role in solute transport. *Protoplasma* 113, 33–43. <https://doi.org/10.1007/BF01283037>

Porter, G.A., Knieval, D.P., Shannon, J.C., 1985. Sugar Efflux from Maize (*Zea mays* L.) Pedicel Tissue. *Plant Physiology* 77, 524–531. <https://doi.org/10.1104/pp.77.3.524>

Radchuk, V., Borisjuk, L., 2014. Physical, metabolic and developmental functions of the seedcoat. *Frontiers in Plant Science* 5. <https://doi.org/10.3389/fpls.2014.00510>

Sosso, D., Luo, D., Li, Q.-B., Sasse, J., Yang, J., Gendrot, G., Suzuki, M., Koch, K.E., McCarty, D.R., Chourey, P.S., Rogowsky, P.M., Ross-Ibarra, J., Yang, B., Frommer, W.B., 2015. Seed filling in domesticated maize and rice depends on SWEET-mediated hexose transport. *Nature Genetics* 47, 1489–1493. <https://doi.org/10.1038/ng.3422>

Thiel, J., Weier, D., Sreenivasulu, N., Strickert, M., Weichert, N., Melzer, M., Czauderna, T., Wobus, U., Weber, H., Weschke, W., 2008. Different Hormonal Regulation of Cellular Differentiation and Function in Nucellar Projection and Endosperm Transfer Cells: A Microdissection-Based Transcriptome Study of Young Barley Grains. *Plant Physiology* 148, 1436–1452. <https://doi.org/10.1104/pp.108.127001>

Thorne, J.H., 1985. Phloem Unloading of C and N Assimilates in Developing Seeds. *Annual Review of Plant Physiology* 36, 317–343. <https://doi.org/10.1146/annurev.pp.36.060185.001533>

van Bel, A.J.E., Hess, P.H., 2008. Hexoses as phloem transport sugars: The end of a dogma? *Journal of Experimental Botany* 59, 261–272. <https://doi.org/10.1093/jxb/erm294>

Wang, E., Wang, J., Zhu, X., Hao, W., Wang, L., Li, Q., Zhang, L., He, W., Lu, B., Lin, H., Ma, H., Zhang, G., He, Z., 2008. Control of rice grain-filling and yield by a gene with a potential signature of domestication. *Nature Genetics* 40, 1370–1374. <https://doi.org/10.1038/ng.220>

Wang, H.L., Offler, C.E., Patrick, J.W., 1995. The cellular pathway of photosynthate transfer in the developing wheat grain. II. A structural analysis and histochemical studies of the pathway from the crease phloem to the endosperm cavity. *Plant, Cell & Environment* 18, 373–388. <https://doi.org/10.1111/j.1365-3040.1995.tb00373.x>

Wang, H.L., Offler, C.E., Patrick, J.W., 1994. Nucellar projection transfer cells in the developing wheat grain. *Protoplasma* 182, 39–52. <https://doi.org/10.1007/BF01403687>

Wang, H.L., Patrick, J.W., Offler, C.E., Wang, X.-D., 1995. The cellular pathway of photosynthate transfer in the developing wheat grain. III. A structural analysis and physiological studies of the pathway from the endosperm cavity to the starchy endosperm. *Plant, Cell & Environment* 18, 389–407. <https://doi.org/10.1111/j.1365-3040.1995.tb00374.x>

Wu, X., Liu, J., Li, D., Liu, C.-M., 2016. Rice caryopsis development I: Dynamic changes in different cell layers. *Journal of Integrative Plant Biology* 58, 772–785. <https://doi.org/10.1111/jipb.12440>

Wu, Y., Lee, S.-K., Yoo, Y., Wei, J., Kwon, S.-Y., Lee, S.-W., Jeon, J.-S., An, G., 2018. Rice Transcription Factor OsDOF11 Modulates Sugar Transport by Promoting Expression of Sucrose Transporter and SWEET Genes. *Molecular Plant* 11, 833–845. <https://doi.org/10.1016/j.molp.2018.04.002>

Yang, X., Wu, F., Lin, X., Du, X., Chong, K., Gramzow, L., Schilling, S., Becker, A., Theißen, G., Meng, Z., 2012. Live and Let Die - The Bsister MADS-Box Gene OsMADS29 Controls the Degeneration of Cells in Maternal Tissues during Seed Development of Rice (*Oryza sativa*). *PLOS ONE* 7, e51435. <https://doi.org/10.1371/journal.pone.0051435>

Yin, L.-L., Xue, H.-W., 2012. The MADS29 Transcription Factor Regulates the Degradation of the Nucellus and the Nucellar Projection during Rice Seed Development. *The Plant Cell* 24, 1049–1065. <https://doi.org/10.1105/tpc.111.094854>

Zee, S.-Y., O'Brien, T.P., 1970. Studies on the Ontogeny of the Pigment Strand in the Caryopsis of Wheat. *Australian Journal of Biological Sciences* 23, 1153–1172. <https://doi.org/10.1071/bi9701153>

Zheng, Y., Wang, Z., 2011. Contrast observation and investigation of wheat endosperm transfer cells and nucellar projection transfer cells. *Plant Cell Reports* 30, 1281–1288. <https://doi.org/10.1007/s00299-011-1039-5>

Zheng, Y., Xiong, F., Wang, Z., Gu, Y., 2015. Observation and investigation of three endosperm transport tissues in sorghum caryopses. *Protoplasma* 252, 705–714. <https://doi.org/10.1007/s00709-014-0705-1>

Figure labels

Fig. 1: Caryopsis Endosperm Assimilate Acquisition Route (CEAAR) models. The models illustrate how resources are mobilized into the endosperm of grass caryopsis.

Fig. 2: Development of Brachypodium distachyon grain post-phloem assimilate transport pathway. (a) Transverse section of a Brachypodium grain at 10 days post anthesis (DPA). Red square indicates area magnified in subsequent images. (b), (c), (d), (e), (f), and (g) are sections Brachypodium grain post-phloem assimilate transport route at 5, 10, 15, 20, 25, and 30 DPA respectively. Sieve element-companion cell complex were present in the vascular bundle all sections. There was progressive accumulation of dark deposits in the pigment strand as the grain develops. Cell death and disintegration of nucellar projection cells closest to the endosperm was observed from 10 DPA and is indicated with arrow heads. This created a transient endosperm cavity present at 15 and 20 DPA. The thickness of nucellar epidermis cell wall adjoining the endosperm increased as the grain developed. Bar = 0.1 mm. Al, aleurone cells; TC, tube cell; EC, endosperm cavity; II, inner integument; NE, Mc, mesocarp; nucellar epidermis; NP, nucellar projection; OI, outer integument; PS, pigment strand; En, endosperm; VB, vascular bundle.

Fig. 3: Transmission electron micrographs of transverse sections of developing Brachypodium grains. (a) Vascular bundle at 20 DPA. Note the prominent nucleus and presence of numerous mitochondria (M) in the dense cytoplasm of the vascular parenchyma (VP) cells. Enuclate sieve elements (SE) are also present. Bar = 5 μ m. (b) Shows chloroplasts (CL) in photosynthetic mesocarp cells followed by tube cells (TC), outer integument (OI), inner integument (II), and nucellar epidermis (NE). Thick deposits of cutin on the outer integument cell walls adjoining cross cells is with arrow heads. Bar = 10 μ m. (c) Nucellar projection (NP) cells nearest the pigment strand (PS) have dense cytoplasm at 20 DPA. Bar = 5 μ m. (d) Mitochondria is present in pigment strand cells whether dark deposits (DD) occur in those cells or not. Bar = 2 μ m. (e) A section through adjacent inner integument cell and a nucellar epidermis cell. Note the prominent plasmalemma between the cells. The cell wall of the nucellar epidermis cell has rich deposit of cellulose indicated with arrow heads. Bar = 2 μ m. (f) At 30 DPA, the nucellar projection has dense cytoplasm and massive cell walls with frequent plasmodesmata connections (indicated with arrow heads). Bar = 5 μ m.

Fig. 4: Delineation of assimilate transport route into Brachypodium endosperm using 5(6)-carboxyfluorescein diacetate (CFDA). (a), (b), (c), and (d) are free hand transverse section of 20 DPA Brachypodium grains. (a) and (b) shows ventral and lateral portions of sections that were incubated for 15 min in distilled water as control. There is auto fluorescence in the epicarp (Ec). (c) and (d) are similar portions of sections made from grains that were incubated in for 15 min in 0.01% CFDA. The dye signal is distinct in the vascular bundle (VB), nucellar projection (NP), nucellar epidermis (NE), and endosperm (En). Bar = 0.05 mm.

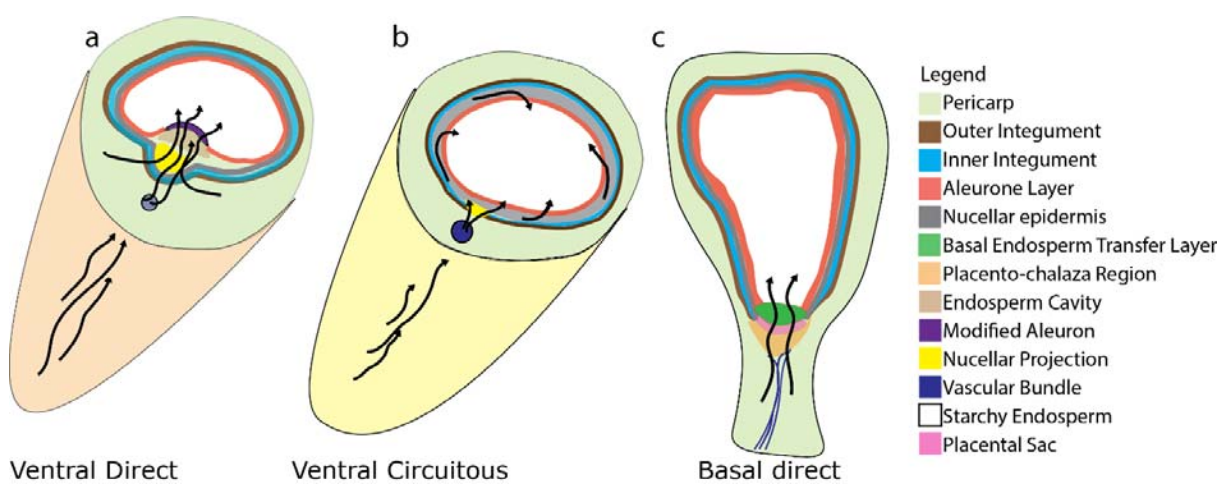


Fig 1

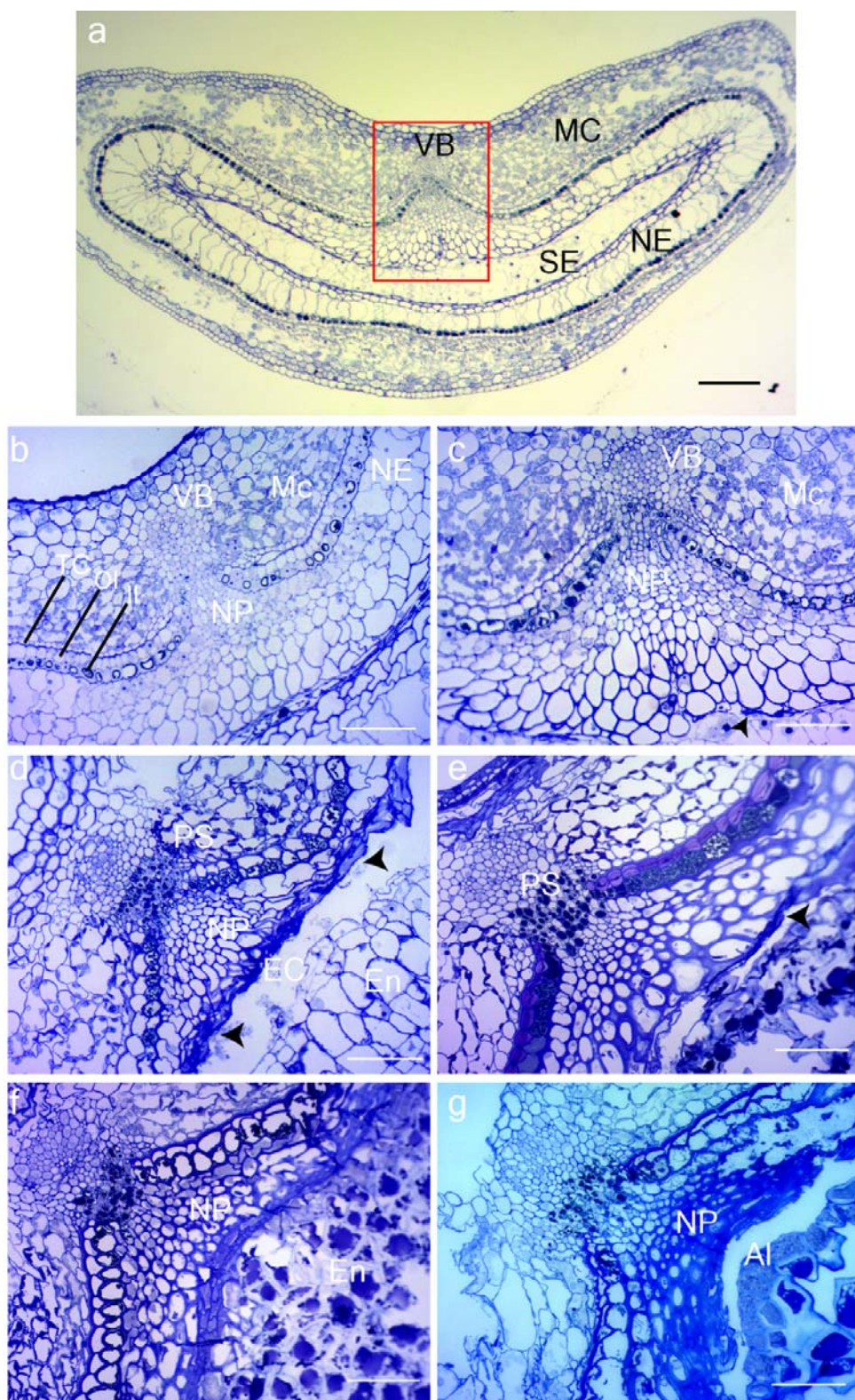


Fig 2

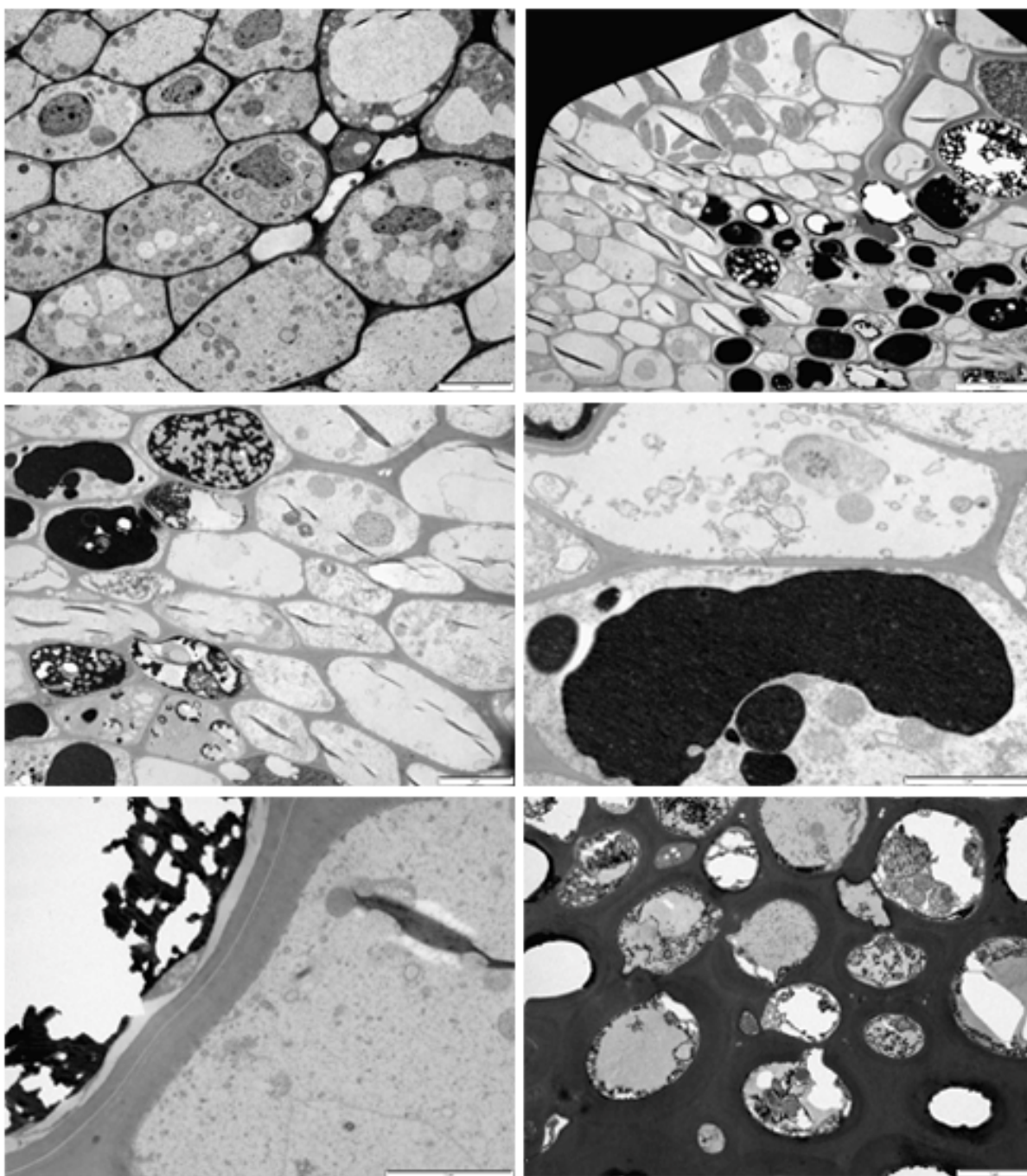


Fig 3

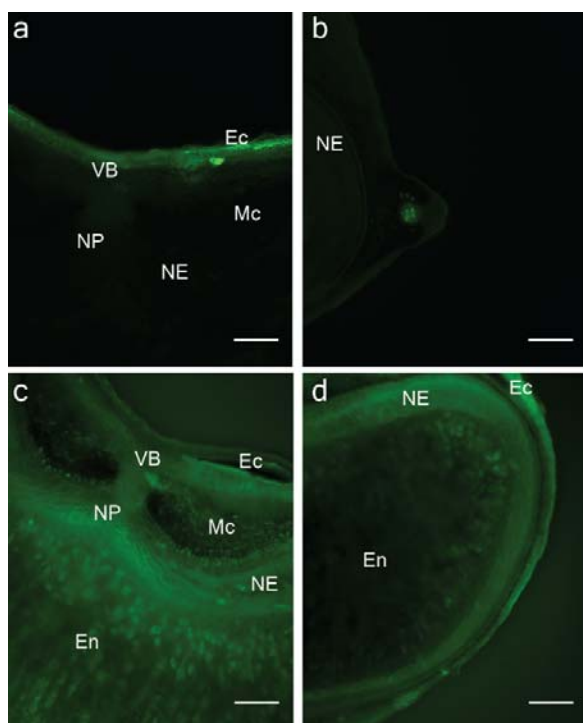


Fig 4.